GEOLOGY | THE GEOLOGICAL SOCIETY OF AMERICA®

https://doi.org/10.1130/G52329.1

Manuscript received 22 April 2024
Revised manuscript received 31 May 2024
Manuscript accepted 5 June 2024

Published online 28 June 2024

Downward continued ocean bottom seismometer data show continued hydrothermal evolution of mature oceanic upper crust

Lianjun Li[1,*], Jenny Collier[1], Tim Henstock[2], and Saskia Goes[1]
[1]Department of Earth Science and Engineering, Imperial College London, SW7 2BP London, UK
[2]School of Ocean and Earth Science, University of Southampton, SO14 3ZH Southampton, UK

ABSTRACT

Heat flow measurements indicate hydrothermal activity in oceanic crust continues at least for 65 m.y. after formation. Hydrothermal activity progressively fills cracks and pores with alteration products, which is expected to lead to a trend of increasing seismic velocities with age. Compilations of seismic-*P*-wave velocity models inverted from ocean bottom seismometer (OBS) data have failed to detect such an aging trend beyond crustal ages of ca. 10 Ma. However, in these models, the velocities of the uppermost crust, where fluid flow would be most concentrated, are poorly resolved. This is because as the oceanic crust matures, the first crustal arrivals on OBS records (which best resolve upper crustal velocities using tomographic inversion), become hidden in the coda of the water wave. This may lead to the masking of any aging trend in the seismic velocities. For the first time, we show how including downward continuation (DC) in the analysis of OBS data collected across 65 Ma seafloor significantly improves measurements of the *P*-wave velocities of the upper crust. Our new analysis reveals a highly heterogeneous upper crust, with ridge-parallel *P*-wave velocity variations of 25%, implying local porosity values that are up to double that of global averages. Our new results, combined with other most recent advanced seismic analyses, reveal that seismic velocities indeed evolve with age up to at least 70 Ma, confirming that hydrothermal activity continues in mature oceanic crust.

INTRODUCTION

Two-thirds of Earth's surface is underlain by oceanic crust, which undergoes geochemical exchange through the hydrothermal circulation of seawater (Fig. 1A; Elderfield and Schultz, 1996). This fluid-rock interaction plays a key role in regulating seawater chemistry and several global chemical budgets (e.g., Nielsen et al., 2006; Coogan and Gillis, 2013). The porous upper oceanic crust is a significant potential reservoir of microbial life, which further influences global-scale biogeochemical cycles (Seyler et al., 2021). To date, the best-understood part of the hydrothermal system is at the mid-ocean ridge axis and flanks (ocean floor ages of <10 Ma), where focused discharge forms spectacular features like black smokers and carbonate chimneys (Beaulieu et al., 2013). However, such features only account for approximately one-third of the total hydrothermal flux. The rest is attributed to more diffuse flow of cooler seawater in more mature oceanic crust (e.g., Hasterok et al., 2011). Here, as the deposition of impermeable marine sediments starts to impede vertical fluid flow, basement highs become increasingly important conduits for hydrothermal fluids (Fisher and Wheat, 2010).

Global marine heat flow compilations suggest hydrothermal heat transfer has largely ceased at crustal ages of ca. 65 Ma (Stein and Stein., 1994). Regional heat flow and cross-borehole studies (e.g., Bartetzko, 2005; Fisher and Von Herzen, 2005), however, provide evidence for hydrothermal activity even in crust older than 100 Ma, suggesting there may be no cessation in hydrothermal circulation with seafloor age (Von Herzen, 2004). Hydrothermal circulation is thought to be increasingly hampered by the blocking of pores/fractures by mineral precipitation, leading to reduced porosity. However, mature basaltic samples are scarce, and macro-porosity is not representatively sampled by drilling (Teagle et al., 2023). Alternative geophysical methods such as natural radioactivity and electrical resistivity offer a more direct link to the crust's physical properties but are too limited to establish age relationships (Bartetzko, 2005). Hence, evidence for the porosity evolution of the upper oceanic crust has relied on wide-angle data collected using ocean-bottom seismometers (OBS). However, thus far, global compilations of wide-angle seismic results have failed to detect systematic increases in velocity expected from porosity reduction, beyond 10 Ma (Grevemeyer and Weigel, 1996; Carlson, 1998; Christeson et al., 2019). Recent long-offset multi-channel seismic reflection (MCS) work in the South Atlantic Ocean (Fig. 1B), however, has shown an evolution of uppermost crustal velocity for at least 48 m.y. or even 63 m.y. (Estep et al., 2019; Kardell et al., 2019, 2021), prompting the need to re-examine OBS data.

One of the biggest challenges for OBS seismology is to constrain *P*-wave velocity (Vp) of the uppermost crustal layers. As the crust ages due to thermal subsidence and sedimentation (Fig. 1C), the source-receiver offset at which the upper crustal refractions (Pg2) become first arrivals (allowing them to be confidently picked) increases (Fig. 1D). Because offset correlates with the depth at which the refracted waves turn, this lack of picks can preclude updating of the starting velocity model for the upper crust used in travel-time tomography. Starting models themselves are typically based on one-dimensional (1-D) crustal *P*-wave velocity-depth profiles below the basement, which are guided by global compilations (e.g., Christeson et al., 2019). Therefore, while conventional wide-angle seismology can effectively determine the bulk crustal structure, the uppermost crust, where physical property changes due to ongoing hydrothermal activity should be most apparent, is the least well-determined part of the crust.

One way to mitigate the deterioration of upper-crustal resolution with age would be to physically place the seismic shots used in the experiments closer to the seabed receivers. While this has been attempted, it has not been widely adopted as a practical way to collect seismic data

Lianjun Li https://orcid.org/0000-0002-7036-0226
*l.li21@imperial.ac.uk

CITATION: Li, L., et al., 2024, Downward continued ocean bottom seismometer data show continued hydrothermal evolution of mature oceanic upper crust: Geology, v. XX, p. , https://doi.org/10.1130/G52329.1

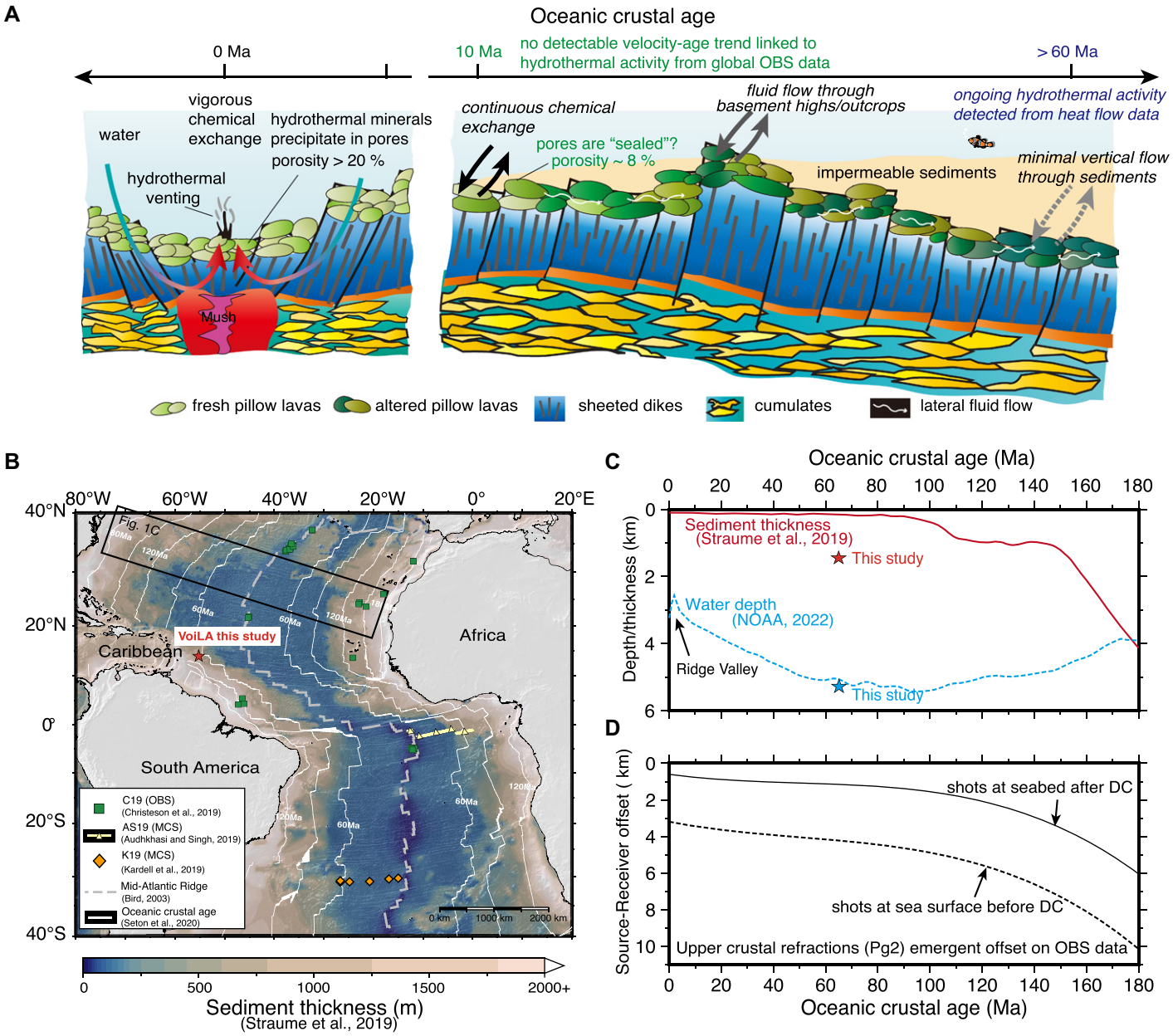

Figure 1. (A) Cartoon illustrating the evolution of oceanic crust formed at a slow-spreading ridge, adapted after Coggon and Teagle (2011) and Fisher and Wheat (2010). (B) Map of sediment thickness and crustal age for the central Atlantic Ocean. Colored symbols mark sites of the data plotted in Figure 4D. Red star is our study region (VoiLA—Volatile Recycling in the Lesser Antilles). (C) Smoothed bathymetry (blue dashed line) and sediment thickness (red solid line) with age averaged within the region marked in B. Red and blue stars are values in our study region. (D) Comparison of the offset at which the upper crustal refraction (Pg2) emerges from the water wave on ocean bottom seismometer (OBS) data with age if the shots are at the sea surface (dashed) and at the seabed (solid). The trends were forward modeled using the data shown in C, and velocities from Christeson et al. (2019). DC—downward continuation; MCS—multi-channel seismic reflection.

(e.g., Sohn et al., 2004). An alternative approach that could, in theory, be applied to seismic data sets is to use a computational method known as downward continuation (DC; Berryhill, 1979) which simulates what would be recorded with shots at depth, collapsing water waves and bringing Pg2 to nearer offsets (Fig. 1D). This approach has been successfully applied to MCS data (e.g., Arnulf et al., 2011; Harding et al., 2016; Kardell et al., 2019) where both the physical source and receiver are at the sea surface, but not, to our knowledge, to OBS data for travel-time tomography. OBS data are generally collected with larger (3 × or more) shot spacing than MCS data, and because the application of DC requires data free of spatial aliasing, this limitation needs to be overcome to apply the method.

We illustrate ways to incorporate DC into the conventional workflow of wide-angle data. We compare Vp models obtained with and without DC application to evaluate accuracy and resolution benefits. Finally, we combine our results from the western Atlantic with other recent studies using advanced analysis to determine if there is a detectable change in seismic properties consistent with heat-flow predictions of hydrothermal activity in mature oceanic crust.

METHODS

We applied our new DC workflow to data collected in 2017 in the western central Atlantic Ocean (Fig. 1B). The oceanic crust there is ca. 65 Ma and is at a depth of ~7 km beneath ~1.5 km of sediment. Figure 2 shows the transformation of an OBS record after DC. DC has collapsed the direct water wave (W) such that the sediment (Ps) phase now becomes a first arrival and the offset at which the upper crustal

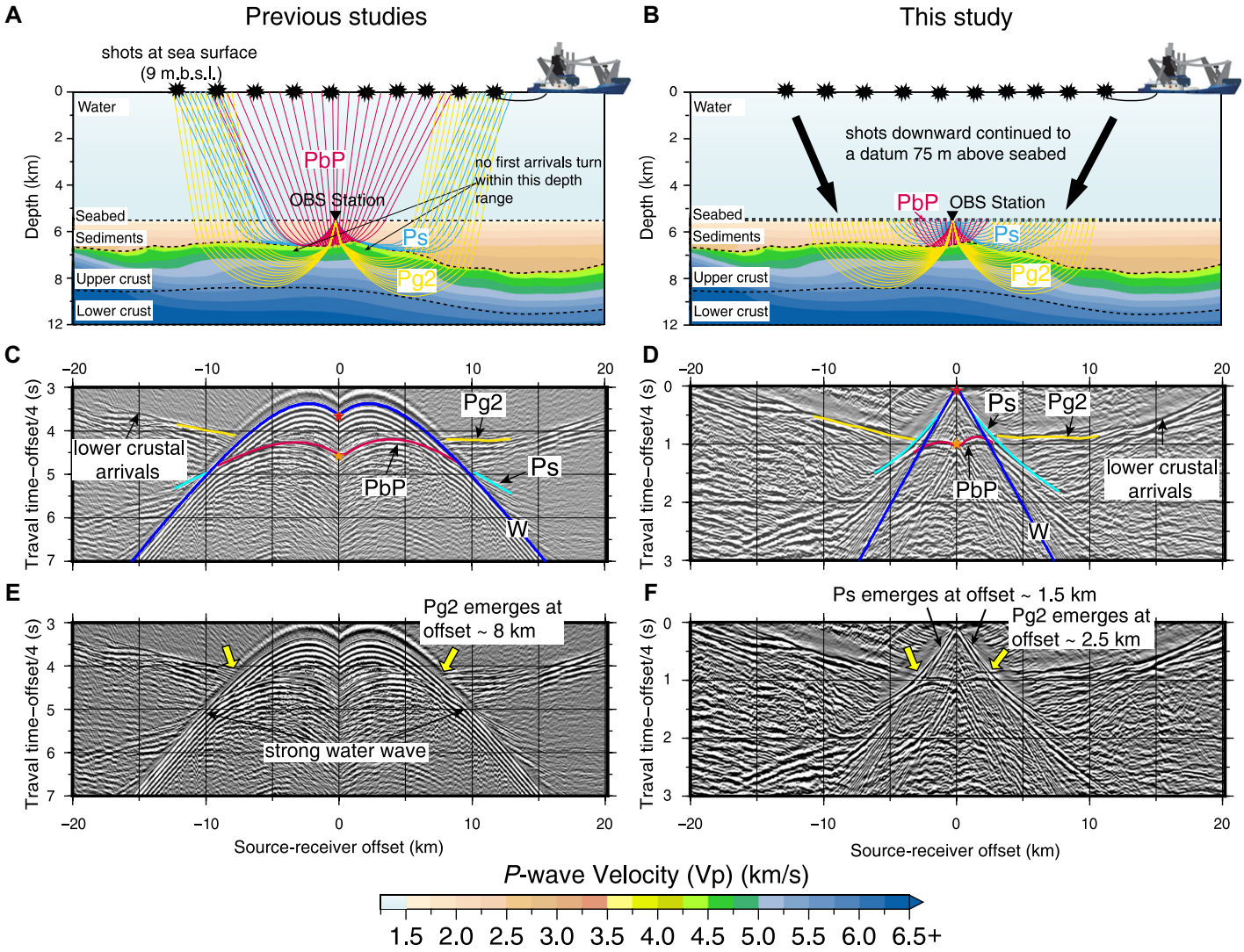

Figure 2. Comparison of the ray geometry and data before (left) and after (right) downward continuation (DC) of an ocean bottom seismometer (OBS) record from the western central Atlantic Ocean. The upper panels show the ray diagram (A, B), the lower two panels show the OBS data with (C, D) and without (E, F) the predicted arrivals. m.b.s.l.—meters below sea level; cyan—sedimentary refractions (Ps); red—reflections from top basement (PbP); yellow—upper crustal refractions (Pg2); blue—water waves; red and orange stars—sea bed and top basement, respectively, picked from multi-channel seismic reflection (MCS).

(Pg2) phase becomes a first arrival reduces from 8 km to 2.5 km.

To illustrate the potential of DC to improve the accuracy of upper crustal Vp structure, we selected 29 OBS deployed across two seafloor spreading segments on either side of the Marathon Fracture Zone (MFZ, 13°36'–14°36'N; Fig. 3A). We deliberately chose these two segments (labeled A and B) as they have velocity-depth characteristics indicating magmatically robust seafloor spreading and are free of anomalous structures like oceanic core complexes (Davy et al., 2020; Fig. S7 in the Supplemental Material[1]).

After picking, travel-time tomographic inversion was performed using TOMO2D (Korenaga et al., 2000) in a top-down manner: first for the sedimentary model using Ps and PbP phases, and next for the upper crustal model using the Pg2 phase. We used the same inversion approach as that described by Davy et al. (2020) but applying DC before picking results in the inclusion of smaller-offset arrivals. See the Supplemental Material for more details.

COMPARISON OF *P*-WAVE MODELS

Figure 3 compares the non-DC and DC model results from which the improved resolution and accuracy can be assessed. In the DC model, the sediments have a high vertical velocity gradient (VVG) of >0.8 s^{-1} above a more gradual <0.4 s^{-1} layer. This corresponds to the known regional sedimentary character where ~800-m-thick chaotic continent-derived Pleistocene (2 Ma) mass-transport deposits lie above more-layered pelagic sediments (Pichot et al., 2012). This subdivision is not present in the non-DC model (Fig. S10), largely because of limited Ps picks from the original OBS records (Fig. 2). In the crust, the Vp of 4.75 km/s in the uppermost crust of the non-DC model is little modified from the starting model (Davy et al., 2020), resulting in much smaller ridge-parallel variations than the DC model. Without the collapse of the water wave, the number of picks for Pg2 phase is 40% lower (Table S3). Although in the non-DC model this upper crustal zone is still crossed by parallel rays that turn deeper down (steeply down or up), only an average velocity over this depth range can be resolved. Without DC picks, Vp resolution is reduced and the Vp uncertainty for the upper crust is ~40% larger (Figs. S16 and S17).

[1]Supplemental Material. Discussion of the downward continuation of OBS data (Figs. S1–S6) and subsequential tomographic inversion of VoiLA Line 2/3 (Figs. S7–S18 and Tables S1–S3). Please visit https://doi.org/10.1130/GEOL.S.26017699 to access the supplemental material; contact editing@geosociety.org with any questions.

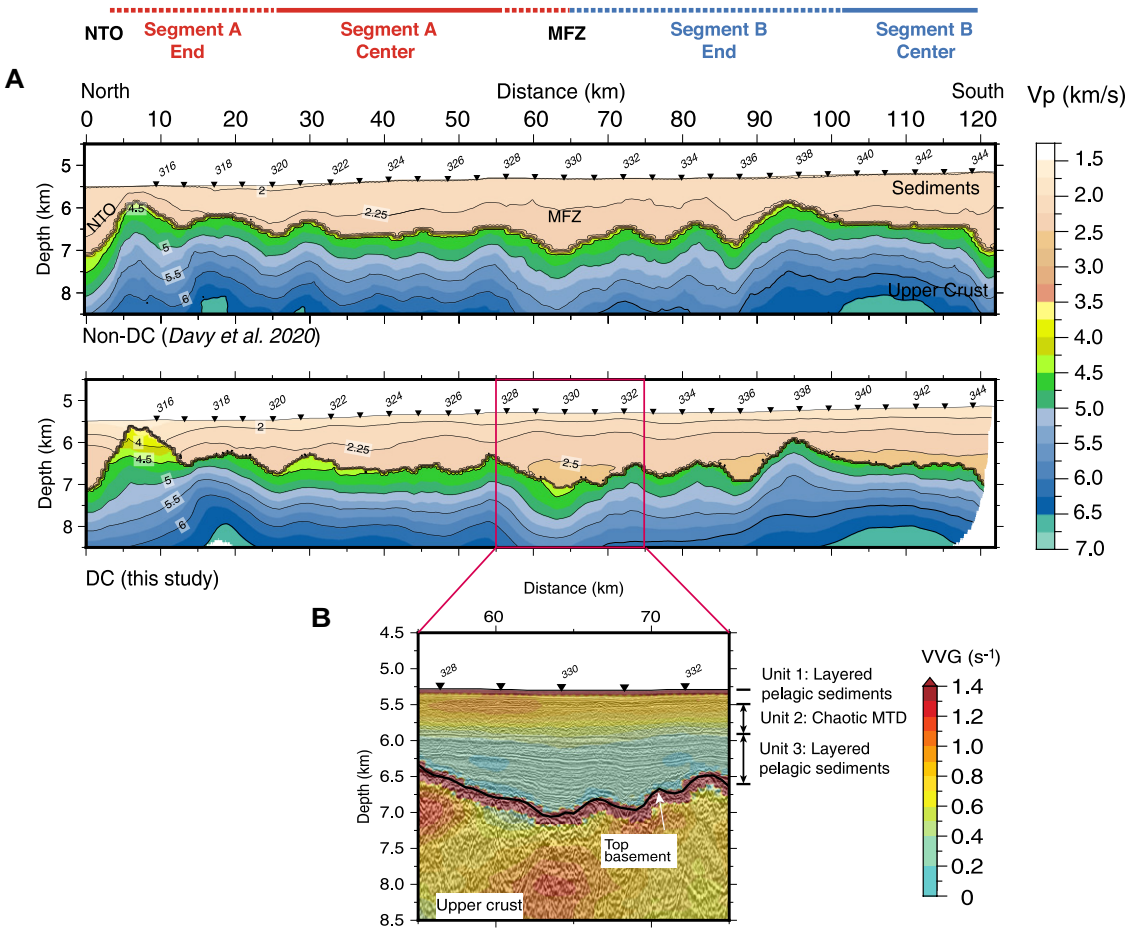

Figure 3. (A) *P*-wave velocity (Vp) models of the Marathon Fraction Zone (MFZ) without downward continuation (non-DC, top) and with DC (bottom). Seafloor spreading segments are from Davy et al. (2020). NTO—non-transform offset. (B) Time-to-depth converted multi-channel seismic reflection image underlain by vertical velocity gradient (VVG) of the DC model. Note the good correlation between VVG and seismic facies. MTD—mass transport deposits.

VARIATION IN UPPER CRUSTAL STRUCTURE

The ridge-parallel variability of the upper crust is highlighted in the VVG and Vp anomaly (Figs. 4A and 4B). The MFZ and Segment B End display a more uniform VVG than the two segment centers, which could be due to more intense fracturing (e.g., Canales et al., 2000), although the northern end of Segment A has a non-uniform VVG. The segment centers have a three-layer VVG, which increases from ~0.4–1.3 s^{-1} within the top 250–600 m, maintains over 1.3 s^{-1} in the subsequent 600 m, and then decreases to 0.2–0.4 s^{-1}. Similar structures have been seen in other magma-robust settings where they have been attributed to changes in volcanic morphology, such as the emergence of dikes or a transition to more massive lava flows (e.g., Christeson et al., 2012).

Both segment Vp averages are below (0.6 km/s and 0.3 km/s lower for Segment A and B, respectively) the global average for mature slow-spreading oceanic crust (Fig. S18A; Christeson et al., 2019). The segmental difference may stem from varying lithologies, which are challenging to discern solely from Vp. Our preliminary *S* wave analysis, however, suggests lithology plays a negligible role for these two magmatic segments. Although we cannot rule out entirely that lithology contributes to the lateral heterogeneity here, the difference in Vp can more readily be interpreted as a difference in porosity. Using the relationships of Carlson (2014) to calculate porosity from seismic velocities gives values of ~16% and 12% for the upper crust in Segments A and B, respectively (Fig. 4D; Fig. S18B), both of which are approximately double that calculated by taking the global average from Christeson et al. (2019) for mature oceanic crust.

Multi-beam bathymetry along the profile shows several small areas of basement outcrop at seabed (Fig. 4C). Some of the basement highs have only recently been buried by sediments (Pichot et al., 2012). With long-term exposure to seawater, these outcrops have likely facilitated ongoing hydrothermal alteration of the upper crust through lateral fluid flow despite most of the crust being under thick and impermeable sediments (Fisher and Wheat, 2010). Our results suggest that mature upper oceanic crust certainly remains porous enough to allow hydrothermal flow. Open cracks in scales detected by the seismic refraction data may persist, as they might not have been effectively sealed by increasing sediments and mineral precipitation. The strong ridge-parallel heterogeneity in crustal structure we observed most likely results from porosity variations due to both different ridge-axis construction and off-axis long-term alteration histories.

IMPLICATION FOR CRUSTAL EVOLUTION

Our analysis suggests that no seismic-velocity-age relationships could be detected for mature crust from previous OBS data compilations because of experimental limitations. Starting models used in travel-time tomography are often guided by global compilations or 1-D fits. Velocities within the upper crustal layer are poorly updated during the inversion process because the shallow turning energy is masked by the water wave (Fig. 1D). The error introduced would increase with age due to thermal subsidence and sedimentation, except in a few cases adjacent to continental margins. For young crust (<10 Ma), where the evolutionary signal is strong and the velocity model is less affected by the sediment burial and the lack of illumination issue, a pattern consistent with ongoing hydrothermal circulation and alteration was clearly seen. Only now, with higher-resolution seismic data, a better understanding of magma-rich and magma-poor seafloor spreading at slow spreading rates, and advanced techniques such as full-waveform inversion and DC, are the errors reduced sufficiently to discern aging patterns in older crust. When combined

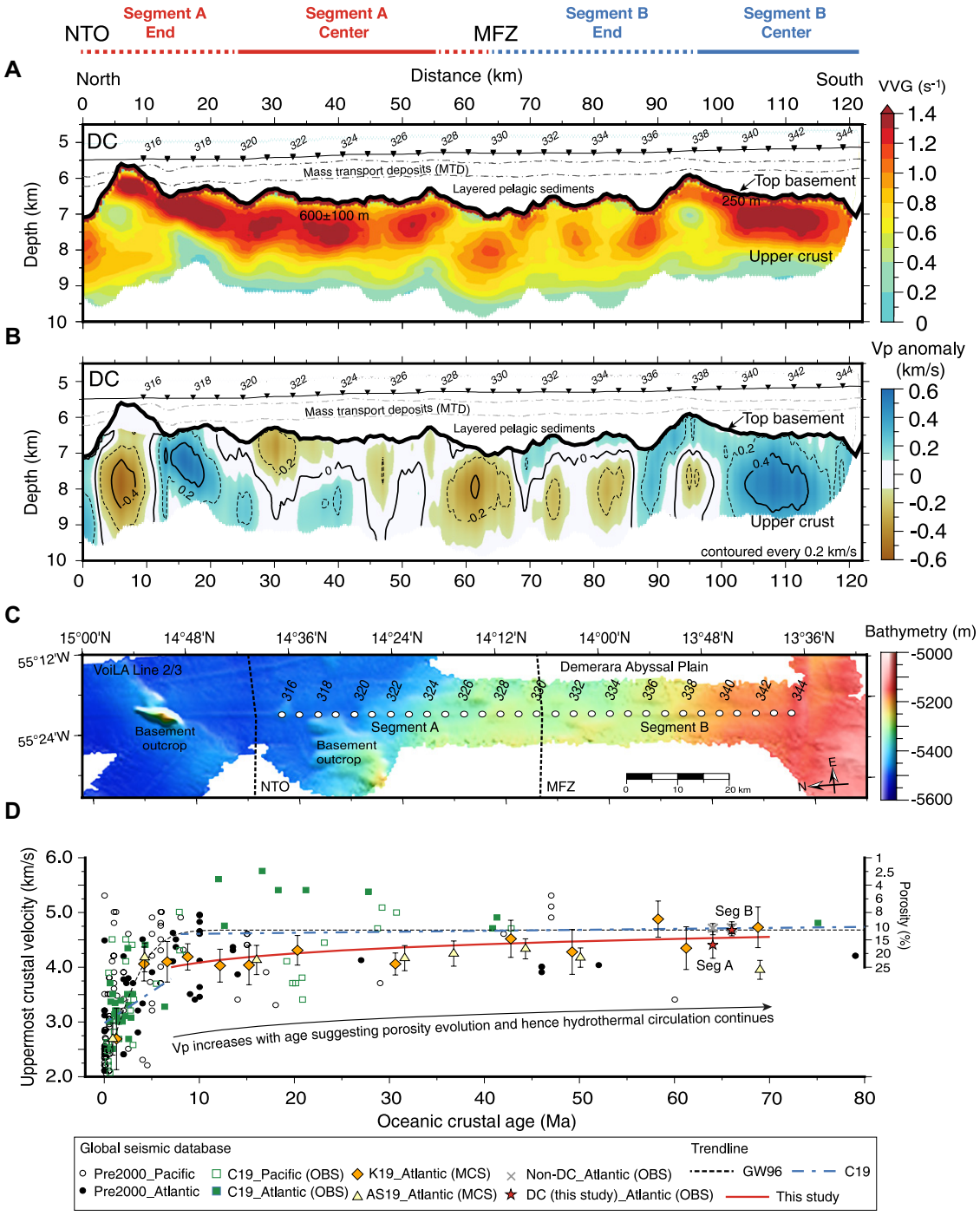

Figure 4. Vertical velocity gradient (VVG) (A) and Vp anomaly (B) computed by subtracting the averaged one-dimensional velocity depth profile from the downward continuation (DC) model. The gray dashed lines outline the sedimentary mass transport deposits (MTD) unit picked from multi-channel seismic reflection data (MCS). (C) Kongsberg-Simrad EM120 multibeam bathymetry showing ocean bottom seismometer (OBS) locations (white circles) and basement outcrops in the region with magnetics-derived seafloor spreading fabric (Davy et al., 2020). VoiLA—Volatile Recycling in the Lesser Antilles; MFZ—Marathon Fraction Zone; NTO—non-transform offset. (D) Compilations of published uppermost crustal Vp against oceanic crustal age plus our two new data points (red stars). Porosity was estimated from Vp following Carlson (2014). The new trendline (red) was calculated from the combined results from this study and those from Kardell et al. (2019) and Audhkhasi and Singh (2019). Older age trends and data points are shown for reference. Data points for both Pacific and Atlantic: Pre2000: Grevemeyer and Weigel (1996) (GW96); Carlson (1998) and Grevemeyer et al. (1999). C19: Christeson et al. (2019). Data points for Atlantic only: K19: Kardell et al. (2019). AS19: Audhkhasi and Singh (2019). Non-DC: Davy et al. (2020).

with two recent Atlantic studies (Fig. 4D; Audhkhasi and Singh, 2019; Kardell et al., 2019), our results support the extension of the trend where Vp increases with age out to ca. 70 Ma. The age trend is visible despite the scatter due to the inherited spatially variable porosity distribution and its modification during aging. Assuming the increase in Vp is due to ongoing reduction of porosity by mineral precipitation, the results imply that fluid flow in the mature crust is more variable and pervasive than previously supported by seismic studies alone, and fluid flow continues to crustal ages consistent with other methods such as heat flow and cross-borehole studies (e.g., Bartetzko, 2005; Neira et al., 2016).

Our work presents a new approach to improving the accuracy of seismic-velocity depth profiles in mature oceanic crust. Currently, models of sufficient quality and age range can only be found for the Atlantic. Therefore, it is not possible to resolve systematic differences in the hydrothermal evolution of Pacific and Atlantic crust from current global compilations (Fig. 4D). We conclude that the application of DC to legacy refraction data sets would substantially improve our understanding of upper-crustal properties. Seismic velocities might be useful in shedding new light on global budgets linked to off-axis hydrothermal circulation.

ACKNOWLEDGMENTS

The data used in this study were collected during Natural Environment Research Council (NERC) grant NE/K010743/1 (VoiLA, Volatile Recycling in the Lesser Antilles) with seabed instruments from the UK Ocean-Bottom Instrumentation Facility (OBIF) and the German Instrument Pool for Amphibian Seismology (DEPAS), hosted by the Alfred Wegener Institute Bremerhaven. We acknowledge Halliburton for providing access to SeisSpace®/ProMax® software via a grant to Imperial College London. We thank Gail Christeson, Ingo Grevemeyer, and an anonymous reviewer for their insightful comments. L. Li

is supported by Imperial College London President's Ph.D. Scholarship Scheme.

REFERENCES CITED

Arnulf, A.F., Singh, S.C., Harding, A.J., Kent, G.M., and Crawford, W., 2011, Strong seismic heterogeneity in layer 2A near hydrothermal vents at the Mid-Atlantic Ridge: Geophysical Research Letters, v. 38, L13320, https://doi.org/10.1029/2011GL047753.

Audhkhasi, P., and Singh, S.C., 2019, Seismic structure of the upper crust from 0–75 Ma in the Equatorial Atlantic Ocean on the African Plate using ultralong offset seismic data: Geochemistry, Geophysics, Geosystems, v. 20, p. 6140–6162, https://doi.org/10.1029/2019GC008577.

Bartetzko, A., 2005, Effect of hydrothermal ridge flank alteration on the in situ physical properties of uppermost oceanic crust: Journal of Geophysical Research, v. 110, B06203, https://doi.org/10.1029/2004JB003228.

Beaulieu, S.E., Baker, E.T., German, C.R., and Maffei, A., 2013, An authoritative global database for active submarine hydrothermal vent fields: Geochemistry, Geophysics, Geosystems, v. 14, p. 4892–4905, https://doi.org/10.1002/2013GC004998.

Berryhill, J.R., 1979, Wave-equation datuming: Geophysics, v. 44, p. 1329–1344, https://doi.org/10.1190/1.1441010.

Bird, P., 2003, An updated digital model of plate boundaries: Geochemistry, Geophysics, Geosystems, v. 4, https://doi.org/10.1029/2001gc000252.

Canales, J.P., Detrick, R.S., Lin, J., Collins, J.A., and Toomey, D.R., 2000, Crustal and upper mantle seismic structure beneath the rift mountains and across a nontransform offset at the Mid-Atlantic Ridge (35°N): Journal of Geophysical Research: Solid Earth, v. 105, p. 2699–2719, https://doi.org/10.1029/1999JB900379.

Carlson, R.L., 1998, Seismic velocities in the uppermost oceanic crust: Age dependence and the fate of layer 2A: Journal of Geophysical Research: Solid Earth, v. 103, p. 7069–7077, https://doi.org/10.1029/97JB03577.

Carlson, R.L., 2014, The influence of porosity and crack morphology on seismic velocity and permeability in the upper oceanic crust: Geochemistry, Geophysics, Geosystems, v. 15, p. 10–27, https://doi.org/10.1002/2013GC004965.

Christeson, G.L., Morgan, J.V., and Warner, M.R., 2012, Shallow oceanic crust: Full waveform tomographic images of the seismic layer 2A/2B boundary: Journal of Geophysical Research: Solid Earth, v. 117, B05101, https://doi.org/10.1029/2011JB008972.

Christeson, G.L., Goff, J.A., and Reece, R.S., 2019, Synthesis of oceanic crustal structure from two-dimensional seismic profiles: Reviews of Geophysics, v. 57, p. 504–529, https://doi.org/10.1029/2019RG000641.

Coggon, R.M., and Teagle, D.A.H., 2011, Hydrothermal calcium-carbonate veins reveal past ocean chemistry: Trends in Analytical Chemistry, v. 30, p. 1252–1268, https://doi.org/10.1016/j.trac.2011.02.011.

Coogan, L.A., and Gillis, K.M., 2013, Evidence that low-temperature oceanic hydrothermal systems play an important role in the silicate-carbonate weathering cycle and long-term climate regulation: Geochemistry, Geophysics, Geosystems, v. 14, p. 1771–1786, https://doi.org/10.1002/ggge.20113.

Davy, R.G., Collier, J.S., Henstock, T.J., and The VoiLA Consortium, 2020, Wide-angle seismic imaging of two modes of crustal accretion in mature Atlantic Ocean crust: Journal of Geophysical Research: Solid Earth, v. 125, https://doi.org/10.1029/2019JB019100.

Elderfield, H., and Schultz, A., 1996, Mid-ocean ridge hydrothermal fluxes and the chemical composition of the ocean: Annual Review of Earth and Planetary Sciences, v. 24, p. 191–224, https://doi.org/10.1146/annurev.earth.24.1.191.

Estep, J., Reece, R., Kardell, D.A., Christeson, G.L., and Carlson, R.L., 2019, Seismic Layer 2A: Evolution and thickness From 0- to 70-Ma crust in the slow-intermediate spreading South Atlantic: Journal of Geophysical Research: Solid Earth, v. 124, p. 7633–7651, https://doi.org/10.1029/2019JB017302.

Fisher, A.T., and Von Herzen, R.P., 2005, Models of hydrothermal circulation within 106 Ma seafloor: Constraints on the vigor of fluid circulation and crustal properties, below the Madeira Abyssal Plain: Geochemistry, Geophysics, Geosystems, v. 6, Q11001, https://doi.org/10.1029/2005GC001013.

Fisher, A.T., and Wheat, C.G., 2010, Seamounts as conduits for massive fluid, heat, and solute fluxes on ridge flanks: Oceanography (Washington, D.C.), v. 23, p. 74–87, https://doi.org/10.5670/oceanog.2010.63.

Grevemeyer, I., and Weigel, W., 1996, Seismic velocities of the uppermost igneous crust versus age: Geophysical Journal International, v. 124, p. 631–635, https://doi.org/10.1111/j.1365-246X.1996.tb07041.x.

Grevemeyer, I., Kaul, N., Villinger, H., and Weigel, W., 1999, Hydrothermal activity and the evolution of the seismic properties of upper oceanic crust: Journal of Geophysical Research: Solid Earth, v. 104, p. 5069–5079, https://doi.org/10.1029/1998JB900096.

Harding, A.J., Arnulf, A.F., and Blackman, D.K., 2016, Velocity structure near IODP Hole U1309D, Atlantis Massif, from waveform inversion of streamer data and borehole measurements: Geochemistry, Geophysics, Geosystems, v. 17, p. 1990–2014, https://doi.org/10.1002/2016GC006312.

Hasterok, D., Chapman, D.S., and Davis, E.E., 2011, Oceanic heat flow: Implications for global heat loss: Earth and Planetary Science Letters, v. 311, p. 386–395, https://doi.org/10.1016/j.epsl.2011.09.044.

Kardell, D.A., Christeson, G.L., Estep, J.D., Reece, R.S., and Carlson, R.L., 2019, Long-lasting evolution of Layer 2A in the Western South Atlantic: Evidence for low-temperature hydrothermal circulation in old oceanic crust: Journal of Geophysical Research: Solid Earth, v. 124, p. 2252–2273, https://doi.org/10.1029/2018JB016925.

Kardell, D.A., Zhao, Z., Ramos, E.J., Estep, J., Christeson, G.L., Reece, R.S., and Hesse, M.A., 2021, Hydrothermal models constrained by fine-scale seismic velocities confirm hydrothermal cooling of 7–63 Ma South Atlantic crust: Journal of Geophysical Research: Solid Earth, v. 126, https://doi.org/10.1029/2020JB021612.

Korenaga, J., Holbrook, W.S., Kent, G.M., Kelemen, P.B., Detrick, R.S., Larsen, H.C., Hopper, J.R., and Dahl-Jensen, T., 2000, Crustal structure of the southeast Greenland margin from joint refraction and reflection seismic tomography: Journal of Geophysical Research: Solid Earth, v. 105, p. 21,591–21,614, https://doi.org/10.1029/2000JB900188.

Neira, N.M., Clark, J.F., Fisher, A.T., Wheat, C.G., Haymon, R.M., and Becker, K., 2016, Cross-hole tracer experiment reveals rapid fluid flow and low effective porosity in the upper oceanic crust: Earth and Planetary Science Letters, v. 450, p. 355–365, https://doi.org/10.1016/j.epsl.2016.06.048.

Nielsen, S.G., Rehkamper, M., Teagle, D.A.H., Butterfield, D.A., Alt, J.C., and Halliday, A.N., 2006, Hydrothermal fluid fluxes calculated from the isotopic mass balance of thallium in the ocean crust: Earth and Planetary Science Letters, v. 251, p. 120–133, https://doi.org/10.1016/j.epsl.2006.09.002.

NOAA (National Oceanic and Atmospheric Administration), 2022, ETOPO 2022 15 Arc-Second Global Relief Model, NOAA National Centers for Environmental Information: https://doi.org/10.25921/fd45-gt74 (accessed April 2023).

Pichot, T., Patriat, M., Westbrook, G.K., Nalpas, T., Gutscher, M.A., Roest, W.R., Deville, E., Moulin, M., Aslanian, D., and Rabineau, M., 2012, The Cenozoic tectonostratigraphic evolution of the Barracuda Ridge and Tiburon Rise, at the western end of the North America–South America plate boundary zone: Marine Geology, v. 303–306, p. 154–171, https://doi.org/10.1016/j.margeo.2012.02.001.

Seton, M., Müller, R.D., Zahirovic, S., Williams, S., Wright, N.M., Cannon, J., Whittaker, J.M., Matthews, K.J., and McGirr, R., 2020, A global data set of present-day oceanic crustal age and seafloor spreading parameters: Geochemistry, Geophysics, Geosystems, v. 21, https://doi.org/10.1029/2020GC009214.

Seyler, L.M., Trembath-Reichert, E., Tully, B.J., and Huber, J.A., 2021, Time-series transcriptomics from cold, oxic subseafloor crustal fluids reveals a motile, mixotrophic microbial community: The ISME Journal, v. 15, p. 1192–1206, https://doi.org/10.1038/s41396-020-00843-4.

Sohn, R.A., Webb, S.C., and Hildebrand, J.A., 2004, Fine-scale seismic structure of the shallow volcanic crust on the East Pacific Rise at 9°50′N: Journal of Geophysical Research: Solid Earth, v. 109, B12104, https://doi.org/10.1029/2004JB003152.

Stein, C.A., and Stein, S., 1994, Constraints on hydrothermal heat flux through the oceanic lithosphere from global heat flow: Journal of Geophysical Research: Solid Earth, v. 99, p. 3081–3095, https://doi.org/10.1029/93JB02222.

Straume, E.O., Gaina, C., Medvedev, S., Hochmuth, K., Gohl, K., Whittaker, J.M., Abdul Fattah, R., Doornenbal, J.C., and Hopper, J.R., 2019, GlobSed: Updated total sediment thickness in the world's oceans: Geochemistry, Geophysics, Geosystems, v. 20, p. 1756–1772, https://doi.org/10.1029/2018GC008115.

Teagle, D. A. H., Reece, J., Coggon, R. M., Sylvan, J. B., Christeson, G. L., Williams, T. J., Estes, E. R., and the Expedition 393 Scientists, 2023, Expedition 393 Preliminary Report: South Atlantic Transect 2: International Ocean Discovery Program, https://doi.org/10.14379/iodp.pr.393.2023.

Von Herzen, R.P., 2004. Geothermal evidence for continuing hydrothermal circulation in older (>60 Ma) ocean crust, *in* Davis, E.E., and Elderfield, H., eds., Hydrogeology of the Oceanic Lithosphere: Cambridge, UK, Cambridge University Press, p. 414–450.

Printed in the USA